

doi:10.1016/j.gca.2004.07.025

Incremental vacuum dehydration-decarbonation experiments on a natural gibbsite $(\alpha\text{-Al}(OH_3))$: CO_2 abundance and $\delta^{13}C$ values

NEIL J. TABOR,* and CRAYTON J. YAPP
Department of Geological Sciences, Southern Methodist University, Dallas, TX, 75275-0395 USA

(Received January 22, 2004; accepted in revised form July 1, 2004)

Abstract—Incremental vacuum dehydration-decarbonation experiments were performed at 190°C on chemically "cleaned" aliquots of a gibbsite-dominated, Eocene-age bauxite sample with evolution of CO_2 and H_2O . "Plateau" F (CO_2/H_2O ratios) and $\delta^{13}C$ values of the CO_2 derived from gibbsite were attained over the dehydration interval, $X_{\nu}(H_2) = 0.16$ to 0.67 (i.e., 16 to 67% breakdown of gibbsite). The plateau value of F for gibbsite was 0.0043 ± 0.0003 , while the corresponding $\delta^{13}C$ value of evolved CO_2 was -16.0%. Additional experiments on chemically cleaned aliquots included (1) treatment with a solution of 0.3M Na-Citrate + 0.1M Na-Dithionite and (2) an exchange experiment with 0.1 bar of ^{13}C -depleted CO_2 (-46%) at $105^{\circ}C$ for 64.5 h. Neither of these additional treatments resulted in a measurable perturbation of plateau values of F or $\delta^{13}C$ for CO_2 evolved from gibbsite during dehydroxylation. These results support published work on Holocene samples which suggested that CO_2 occluded in gibbsite may preserve information on $\delta^{13}C$ values of CO_2 in ancient terrestrial systems. The plateau values of F observed in the Eocene gibbsite indicate that it may be possible to experimentally calibrate a relationship between the concentration of CO_2 occluded in gibbsite and CO_2 in the environment at the time of crystallization. Such a calibration would significantly enhance the value of gibbsite as a source of information on ancient oxidized carbon systems. *Copyright* © 2005 *Elsevier Ltd*

1. INTRODUCTION

Gibbsite $(\alpha$ -Al(OH)₃) is a common constituent in low-temperature hydrothermal deposits and saprolites and soils of humid regions around the world (e.g., Valeton, 1972). The potential of gibbsite as a source of information on paleoenvironments is indicated by studies of its hydrogen and oxygen isotope systematics (Bird et al., 1994; Vitali et al., 2000; 2001; Girard et al., 2002). Moreover, Schroeder and Melear (1999) observed that CO₂ was evolved from gibbsite during incremental vacuum dehydration-decarbonation experiments. They found that the δ^{13} C values of sequential increments of this CO2 were relatively invariant (i.e., achieved a plateau) and appeared to reflect the δ^{13} C of the soil CO₂ present during gibbsite crystallization (Schroeder and Melear, 1999). In contrast, the CO₂/H₂O ratios (F-values) of the evolved gases were not constant. Schroeder and Melear (1999) attributed this inconstancy to the variable contributions of water from dehydration of poorly ordered hydroxides and halloysite.

Schroeder and Melear (1999) proposed that CO_2 is occluded in gibbsite and that this CO_2 may provide information on environments of formation in a manner analogous to that of the $Fe(CO_3)OH$ component in goethite. Such information includes the $\delta^{13}C$ of ancient soil ecosystems and concentrations of CO_2 in the soil and global atmosphere (Yapp, 1987; 1996; 1998; 2001; 2002; Yapp and Poths, 1990; 1991; 1992; 1993; 1996). For paleoenvironmental information of this type to be realized from ancient gibbsites, the following conditions must obtain: (1) the CO_2 should be occluded in gibbsite during mineral crystallization, (2) the gibbsite must be closed with respect to the occluded CO_2 (i.e., the occluded CO_2 is non-exchangeable);

(3) the carbon isotope fractionation factor between CO_2 gas and CO_2 occluded in gibbsite must be known; and (4) the equilibrium constant relating the concentration of CO_2 gas to the concentration of CO_2 occluded in the gibbsite should be known. The latter condition requires that the concentration of CO_2 occluded in gibbsite can be measured reproducibly and accurately. To address issue (2) and the second part of (4), incremental vacuum dehydration/decarbonation and carbon isotope exchange experiments were performed on Eocene-age gibbsite-rich samples from a bauxite deposit from central Arkansas, U.S.A.

2. MATERIALS AND METHODS

2.1. Characterization and Chemical Pretreatment

The bauxite that is the subject of this study was taken from the mineral collections in the Department of Geological Sciences at Southern Methodist University. The sample is a hand specimen (~ 60 g) of an Eocene-age bauxite from Saline County, Arkansas, U.S.A. This specimen exhibits a pisolitic texture and likely originated from the "zone of concretion" in a paleosol complex developed upon nepheline syenite (Gordon et al., 1958).

Figure 1 presents a schematic diagram of procedures and chemical treatments of the samples discussed herein. The bauxite sample was initially crushed in a steel-piston device and ground under reagent grade acetone in a corundum mortar and pestle to produce a powder. Powders were then passed through a 63 μm brass sieve. All subsequent discussion refers to the $<63~\mu m$ size fraction of the Eocene-age bauxite. $\sim 3-4~g$ of bauxite sample were treated overnight at room temperature in $\sim 40-50~mL$ of 0.5N HCl to remove carbonate minerals such as calcite and soluble organics. Samples were then washed with successive aliquots of de-ionized H_2O until the pH of the rinse water was equivalent to that of the initial de-ionized H_2O . The bauxite samples were then treated at room temperature with successive aliquot of concentrated H_2O_2 (30% solution) to oxidize organic matter. When the reactivity of an aliquot of H_2O_2 diminished, the supernatant was decanted and a fresh aliquot of H_2O_2 was added to the sample. After 31

^{*} Author to whom correspondence should be addressed (ntabor@ mail.smu.edu).

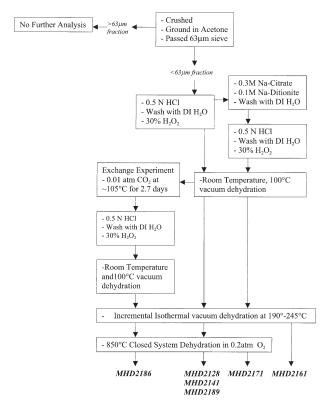


Fig. 1. Flow chart depicting the various analytical procedures employed for different incremental vacuum dehydration-decarbonation experiments. See text for details.

days of H_2O_2 treatment, bauxite samples were dried in a vacuum desiccator at room temperature ($\sim 23^{\circ}\pm 1^{\circ}C$).

Bauxite samples were analyzed by X-ray diffractometry to determine the mineralogical composition and to determine the mineralogical effects, if any, of chemical treatments. X-ray diffraction analyses were performed on a Scintag PADV diffractometer, using $\text{CuK}\alpha$ at 40Kv and 30mA. Measurements were performed with step-scan increments of 0.01° 2 θ , counting times of 10s per increment, 0.5/1.0 mm for the primary slits and 0.2/0.3 mm for the receiving slits.

2.2. Methods of Incremental Dehydration-Decarbonation

Incremental dehydration analyses of the bauxite samples were performed using the method of Yapp and Poths (1991, 1993) and Hsieh and Yapp (1999) as described in the following procedures (see also method of Schroeder and Melear, 1999). Initial masses of the bauxite samples ranged from $\sim\!109$ to 255 mg (Appendix I). Samples were loaded into a quartz reaction chamber and flushed with pure O_2 for 3 min at room temperature. The sample chamber was then evacuated at temperatures of $\sim\!23^\circ\text{C}$ for times ranging from 26 to 165 min, followed by heating at 100°C under open system conditions in vacuum for 30 to 57 min to remove sorbed H_2O and CO_2 .

After the 100°C step, samples were heated under closed system conditions in $\sim\!0.2$ atm O_2 for $\sim\!30$ min at temperatures of 190 or 230°C depending upon the sample (see Appendix) to facilitate oxidation of organic carbon that might have persisted through the H_2O_2 treatment and that might otherwise evolve in subsequent open system vacuum dehydration-decarbonation steps. After evacuation of O_2 and collection of dehydration products from the closed system step, all samples but one were subjected to incremental isothermal open system vacuum dehydration at a temperature of 190°C. The one exception (MHD-2128) was dehydrated at temperatures of 230 to 245 °C. The duration of each open system step ranged from 30 to 1050 min. After the rate of mineralogical breakdown (dehydration) had significantly

diminished, samples were subjected to a final closed system dehydration in ${\sim}0.2$ bar O_2 at $850^{\circ}C$ for ${\sim}30$ min.

The CO_2 and H_2O collected at each step were separated cryogenically. The evolved water was quantitatively converted to H_2 over uranium at $\sim 760^{\circ}C$. Yields of H_2 and CO_2 were measured manometrically. H_2 yield was measured with a precision of about $\pm 1~\mu$ mol. For CO_2 , differences in yield of $\sim 0.1~\mu$ moles could be resolved.

Stable carbon isotope ratios of evolved CO_2 were measured on a Finnigan MAT 252 mass spectrometer, and reported as $\delta^{13}C$, where

$$\delta^{13}C = \left[\frac{R_{\text{sample}}}{R_{\text{standard}}} - 1 \right] \times 1000\%$$
 (1)

 $R={}^{13}\text{C}/{}^{12}\text{C}$. The standard is PDB for $\delta^{13}\text{C}$ analyses (Craig, 1957). Replicate analyses of individual aliquots of CO_2 samples results in a $\delta^{13}\text{C}$ analytical uncertainty for $\delta^{13}\text{C}$ of $\pm~0.3\%$ or better.

2.3. Experimental Outline

The $<63 \mu m$ size fraction of the bauxite sample that had undergone 0.5N HCl and 30% H₂O₂ treatment was split into four fractions. One fraction (MHD-2161) underwent incomplete vacuum dehydration-decarbonation, during open system conditions, at 190°C for 317 min. The residual solids were then removed from the reaction chamber and analyzed by X-ray diffraction to assess mineralogical trends, if any, in the breakdown-process of gibbsite. A second fraction (MHD-2171) was treated with a solution of 0.3M Na-citrate and 0.1M Na-dithionite at room temperature (~23°C) for 2 days to determine the effects of citrate-dithionite treatment on the concentration and δ^{13} C of CO₂ evolved during bauxite dehydration (Fig. 1). After citrate-dithionite (CD) treatment, the sample was rinsed in deionized H₂O and underwent the same set of chemical treatments described in section 2.1 (i.e., 0.5N HCl, H₂O₂, vacuum dehydration). A third fraction (MHD-2186) of bauxite was used in a CO₂ exchange experiment to assess whether CO₂ associated with gibbsite is readily exchangeable. This fraction was "outgassed" at 105°C in vacuum. ~0.10 atm of cryogenically purified tank CO₂ (δ^{13} C = -45.8%) was subsequently introduced into the evacuated dehydration chamber and kept under closed system conditions in contact with this sample (MHD-2186) at 105°C for ~65 h. At the end of that time, the tank CO₂ was removed for measurement of its δ¹³C value. The bauxitic gibbsite was also removed from the dehydration chamber and subjected to a repetition of the set of chemical treatments described in section 2.1 followed by incremental vacuum dehydration-decarbonation. A fourth fraction was subdivided into three aliquots (MHD-2128, MHD-2141 and MHD-2189) which were incrementally dehydrated with no further chemical treatment. One sample from this fourth fraction (MHD-2128) underwent open-system dehydration at 230 to 245 °C, whereas the other two samples were dehydrated under open-system conditions at 190°C. Results of the incremental vacuum dehydration-decarbonation extractions are presented in Appendix 1.

3. RESULTS AND DISCUSSION

3.1. Mineralogy

X-ray diffraction spectra (Fig. 2) of the untreated and various chemically treated bauxite samples are virtually identical, suggesting that the chosen chemical treatments have no gross effect on the bulk mineralogical composition of the bauxite. Sharp and narrow peaks at \sim 4.85Å, 4.37Å, 4.32Å, 2.38Å and 2.05Å correspond to the primary d(hkl) spacings of gibbsite. The intensities of these gibbsite peaks indicate that it is the dominant mineral in the <63 μ m size fraction. The X-ray diffractograms also show low and broad peaks at \sim 7.2Å \sim 6.1Å and \sim 3.6Å, likely corresponding to minor amounts of kaolinite and boehmite (Moore and Reynolds, 1997). No other minerals were positively identified in these samples.

X-ray diffraction analysis of MHD-2161, the bauxite sample that underwent partial vacuum dehydration at 190°C for 317

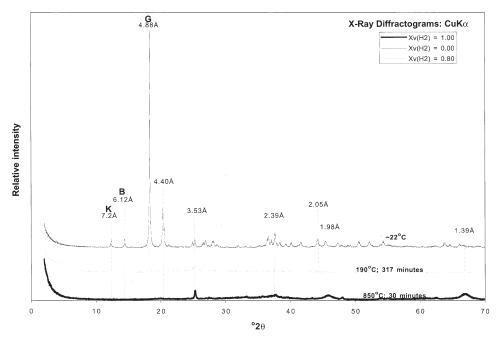


Fig. 2. X-ray diffraction patterns of the <63 μ m fraction Eocene bauxite before incremental vacuum dehydration ($X_v(H_2) = 0.00$), after 317 min of 190°C open system dehydration-decarbonation ($X_v(H_2) = 0.80$) and after 850°C closed system dehydration ($X_v(H_2) = 1.00$). At $X_v(H_2) = 0$, the dominant peaks represent gibbsite (**G**)with subordinate peaks for kaolinite (**K**) and boehmite (**B**). At $X_v(H_2) = 0.80$, peaks from gibbsite remain dominant, but the intensity of the kaolinite (001; **K**) and boehmite (020; **B**) peaks relative to the gibbsite (002) peak become 3.5 times greater than at $X_v(H_2) = 0.00$. At $X_v(H_2) = 1.00$, gibbsite, kaolinite and boehmite have been destroyed. Broad and low peaks correspond to an unidentified material. See Text.

min, shows that gibbsite and kaolinite are the primary mineralogical phases with boehmite as a minor constituent (Fig. 2). However, all of the peaks have significantly lower intensity after the 190°C dehydration, suggesting that much of the original material has been destroyed and the dehydration product may be present as an X-ray amorphous matrix. With respect to the gibbsite (002) peak, the relative intensities of the kaolinite (001) and boehmite (020) peaks are \sim 3.5 times greater after 317 min of 190°C open system dehydration. This probably reflects preferential destruction of gibbsite at 190°C compared to coexisting kaolinite and boehmite (e.g., Rooksby, 1961; Criado et al., 1984). The 850°C-dehydration residue of the bauxite exhibits several low and broad peaks at 3.53Å, 2.39Å, 1.98Å and 1.39Å (Fig. 2). These peaks may correspond to one of the anhydrous, high-temperature dehydration products of gibbsite: χ -Al₂O₃, κ -Al₂O₃, γ -Al₂O₃, θ -Al₂O₃ or α -Al₂O₃ (Paulik et al., 1983).

3.2. Incremental Dehydration-Decarbonation

Results from the bauxite dehydration-decarbonation experiments are reported in Appendix 1. The amount of $\rm CO_2$ from the initial combined outgassing at $\sim\!23^\circ$ and $100^\circ\rm C$ is very low for all samples, ranging from 0.1 to 0.3 μ moles with $\delta^{13}\rm C$ values ranging from -8.2% to -12.8%. With the exception of MHD-2171, all of the samples have very low concentrations of water outgassed at $100^\circ\rm C$ (Appendix 1), ranging from 0.7 to 1.0% of the initial sample mass. This outgassed $\rm CO_2$ and $\rm H_2O$ probably represent gases sorbed on the mineral surfaces.

3.2.1. Gibbsite thermal dehydration temperatures

Schroeder and Melear (1999) performed incremental vacuum dehydration-decarbonation experiments on gibbsite-rich samples from an Ultisol in Georgia, USA. Those workers determined that a rate of gibbsite breakdown permissive of controlled recovery of cryogenically collected increments of evolved CO₂ is achieved under open system conditions at temperatures of 230°-240°C. In the current study, a 230 to 240 °C vacuum dehydration-decarbonation temperature resulted in very rapid (catastrophic) breakdown of the gibbsite that precluded recovery of sufficient numbers of CO2 increments to provide good resolution of the dehydration process (MHD-2128; see Appendix). This is reflected in the kinetic data in Figure 3, which presents values of X_s*(H₂) plotted against cumulative time of isothermal dehydration. X_s*(H₂) represents the mole fraction of total hydrogen in the system that remains in the mineral after each isothermal dehydration step (the initial closed system step in oxygen is not included in the total). At isothermal dehydration-decarbonation temperatures of 230°C, more than 60% of the mineral-bound H₂O was removed after the first 30 min open system step, whereas only 14%-25% of the mineral-bound H₂O is removed after the first open system dehydration step at 190°C (Fig. 3). The slower rate of dehydration at 190°C provides more control and potentially more detailed information on the release of CO2 and H2O during gibbsite breakdown than does the 230°C dehydration experiment (Fig. 3). Therefore, a temperature of ~190°C was em-

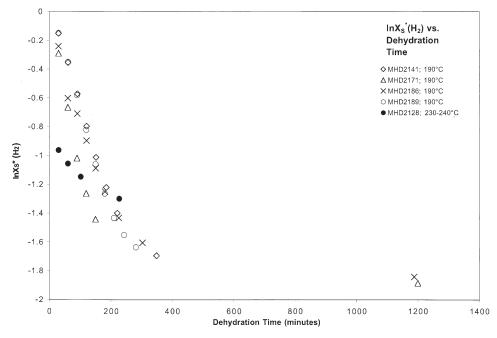


Fig. 3. $X_s*(H_2)$ vs. dehydration time for open system dehydration of bauxite at 190°C and 230°C. The rate of dehydration at 190°C open system conditions in vacuum slows abruptly at $X_s*(H_2)$ values of \sim 0.20.

ployed for the isothermal vacuum dehydration-decarbonation steps.

3.2.2. $0.5M\ HCl + H_2O_2$ -treated Gibbsite

The results from the incremental, isothermal vacuum dehydrations of the bauxite samples treated only with 0.5N HCl + $\rm H_2O_2$ are depicted in the spectra of Figure 4a and b. The progress variable $\rm X_v(H_2)$ is the cumulative sum of evolved $\rm H_2$ as a mole fraction of the total hydrogen in the bauxite sample (exclusive of the $100^{\circ}\rm C$ step). When $\rm X_v(H_2)=0$, there has been no breakdown of the bauxitic minerals. When $\rm X_v(H_2)=1$, the bauxite has been completely dehydrated and, in particular, gibbsite (α -Al(OH)₃) has been completely converted to a nearly amorphous aluminum oxide (Rooksby, 1961; Paulik et al., 1983; Moore and Reynolds, 1997). The "F" parameter in Figure 4a is defined as follows (Yapp and Poths, 1993): F = $\rm n(CO_2)/n(H_2O)$, where $\rm n(CO_2)=\mu mol$ of $\rm CO_2$ evolved in an increment of bauxite dehydration-decarbonation, and $\rm n(H_2O)=\mu mol$ of $\rm H_2O$ evolved over that same increment.

For all of the 190°C experiments (Appendix 1), the open system dehydration-decarbonation increments exhibit a range of F values from 0.0014–0.0052 and a range of δ^{13} C values from -20.8% to -15.0%. For the standard chemical treatment of 0.5N HCl and H_2O_2 used with MHD-2141 and MHD-2189, 190°C open system data collected over the range $X_{\rm V}(H_2)$ = 0.16–0.67 exhibit relatively uniform values of F (avg. = 0.0042 \pm 0.0002 and 0.0043 \pm 0.0003, respectively) and $\delta^{13}C_{\rm CO_2}$ (avg. = $-16.0 \pm 0.4\%$ and $-16.1 \pm 0.4\%$, respectively; Figs. 4a and b, Appendix 1). For reasons that are not apparent at this time, open system F and $\delta^{13}C$ values are more variable for 190°C increments at $X_{\rm v}(H_2)$ values >0.67 (Figs. 4a and 4b, Appendix 1). Therefore, in this paper we employ the operationally defined term "plateau value(s)" to describe the

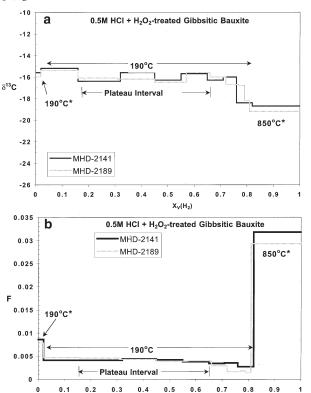


Fig. 4. Incremental dehydration spectra for samples MHD-2141 and MHD-2189, which were treated only with 0.5N HCl and 30% $\rm H_2O_2$ solution. The "plateaus values" in 190°C open-system $\delta^{13}C$ and F values for $\rm CO_2$ evolved over the "plateau dehydration interval" (from $\rm X_v(H_2)=0.16$ to 0.67) are assumed to represent CO_2 occluded in the gibbsite structure (see text). Average plateau $\delta^{13}C_{\rm CO_2}$ values are $-16.0\pm0.4\%e$ and $-16.1\pm0.4\%e$, whereas average plateau F values are 0.0042 ± 0.0002 and 0.0043 ± 0.0003 for MHD-2141 and MHD-2189, respectively.

 $X_v(H_2)$

relatively narrow ranges of F and $\delta^{13}C_{CO2}$ values that characterize gibbsite dehydration in the bauxite samples over the defined "plateau dehydration interval" $X_v(H_2) = 0.16$ to 0.67.

Incremental vacuum dehydration-decarbonation experiments performed on gibbsites from a Holocene-age soil demonstrate that evolved CO₂ can exhibit relatively uniform δ^{13} C values (Schroeder and Melear, 1999). Schroeder and Melear (1999) speculated that this CO₂ component is mineralogically bound to crystal-edge defects within the gibbsite and remains confined until the gibbsite crystal structure is destroyed. Schroeder and Melear (1999) recognized that if their hypothesis is correct, gibbsite dehydration-decarbonation spectra should also exhibit fairly uniform F ratios (nCO₂/nH₂O). However, because of the presence of "nonstoichiometric" water that was evolved from admixed halloysite at the same temperature as gibbsite dehydroxylation, plateau values of F were not observed within any of the incremental dehydration spectra of their soil samples (Schroeder and Melear, 1999). Analyses of the Eocene-age bauxite, which does not contain halloysite, show reproducible plateau values of F and δ^{13} C for MHD-2141 and MHD-2189. These new results appear to support the original hypothesis of Schroeder and Melear (1999). Therefore, we assume that the "plateau" CO2 which is evolved during open system vacuum dehydration-decarbonation of the bauxitic gibbsite in our experiments derives from an isotopically homogeneous, uniformly distributed CO_2 component occluded in the α -Al(OH)₃ crystal structure.

Treatment of samples with a solution of 0.3M Na-Citrate and 0.1M Na-Dithionite (CD-treatment) is a standard chemical procedure for removal of Fe- and Mn-oxides from silicates and Al-oxyhydroxides (modified procedure of Jackson, 1979; see section 2.3.). CD-treatment of bauxite sample, MHD-2171, was designed to determine whether this standard procedure perturbs the plateau values of F and δ^{13} C of CO₂ extracted from gibbsite. Plateau values observed in MHD-2141 and MHD-2189 are used as the reference. The δ^{13} C of the Na-Citrate used for the CD-treatment of MHD-2171 is $-13.2 \pm 0.3\%$ (n = 1). Although the citrate δ^{13} C value is only $\sim 2.8\%$ more positive than the plateau δ^{13} C value of CO₂ from gibbsite, it might be expected that CO2 evolved from citrate-treated gibbsite would exhibit more positive δ^{13} C values and higher F values if the citrate was a source of contaminant CO₂. The plateau values of F and δ^{13} C for MHD-2141 and MHD-2189 define a characteristic area (or "domain") in a plot of δ^{13} C vs. F (Fig. 5a). If CD-treatment had significantly altered the gibbsite in MHD-2171, it is expected that F and δ^{13} C values collected over the plateau interval for this sample would plot outside of the plateau domain.

There are only two open system vacuum dehydration-decarbonation increments collected from MHD-2171 that lie within the range of $X_{\nu}(H_2)$ values corresponding to the plateaus of MHD-2141 and MHD2189. These two increments represent dehydration of the bauxitic gibbsite over the interval $X_{\nu}(H_2)$ = 0.27–0.65 (Fig. 6a and 6b). The F value for MHD-2171 over this range is 0.0043 \pm 0.0002, whereas the $\delta^{13}C_{\rm CO2}$ value is $-16.0 \pm 0.6\%$. The F and $\delta^{13}C_{\rm CO2}$ values for both increments

lie within the plateau domain defined by MHD-2141 and MHD-2189 (Fig. 5b). Thus, plateau F and $\delta^{13}C_{\rm CO2}$ values that define the CO $_2$ occluded in gibbsite are apparently not affected by CD treatment, and such treatment seems to be a reasonable method by which to isolate relatively pure gibbsite from natural samples for evaluation of $\delta^{13}C_{\rm CO2}$ and F values.

3.2.4. Gibbsite-CO₂ exchange experiment followed by 0.5M HCl + H₂O₂-treatment

The CO₂-exchange experiment for sample MHD-2186 was designed to examine possible carbon isotope exchange between CO₂ gas and CO₂ occluded in gibbsite at a relatively warm temperature of 105°C and a CO₂ partial pressure of 0.1 atm. Under these conditions, the gibbsite was mineralogically stable. Moreover, such conditions may approximate some diagenetic and hydrothermal environments to which gibbsite could be exposed subsequent to crystallization. As noted in Section 2.3, MHD-2186 was placed in a chamber with 0.1 atm of cryogenically purified tank CO_2 ($\delta^{13}C = -45.8\%$; n = 2) at $105^{\circ}C$ for 3875 min. MHD-2186 was subsequently removed from the reaction chamber, treated overnight with 0.5M HCl to remove surface-sorbed CO₂, rinsed with deionized H₂O, and treated with 30% H₂O₂ before isothermal, incremental vacuum dehydration-decarbonation. Therefore, if δ^{13} C values of CO₂ evolved during dehydration of MHD-2186 over the X_v(H₂) range 0.16 to 0.67 are more negative than plateau δ^{13} C values determined from MHD-2141 and MHD-2189, they may reflect exchange with the tank CO_2 .

Four open system vacuum dehydration-decarbonation increments from MHD-2186 lie within the reference "plateau interval," $X_{\nu}(H_2)=0.16$ to 0.67 (Fig. 6a and 6b, Appendix 1). These four increments represent dehydration over the interval $X_{\nu}(H_2)=0.23-0.67$. All four pairs of incremental F and $\delta^{13}C_{\rm CO2}$ values from this interval lie within the "plateau domain" defined by MHD-2141 and MHD-2189 (Fig. 5c). The weighted-mean F value (MHD-2186) over this range is 0.0040 \pm 0.0003, whereas the weighted mean $\delta^{13}C_{\rm CO2}$ value is $-16.4\pm0.3\%e$.

Interestingly, the $\delta^{13}C$ values of CO_2 from the $100^{\circ}C$ and closed system $190^{\circ}C$ increments from MHD-2186 are much more negative after the exchange experiment than for samples which were not subjected to exchange (Appendix I). Yet, the fact that the subsequent vacuum dehydration steps for MHD-2186 (within the $X_{\nu}(H_2)$ interval 0.16 to 0.67) exhibit the same plateau values for F and $\delta^{13}C$ as the reference samples indicates the plateau CO_2 is derived from a non-exchangeable, isotopically homogeneous source of carbon, with $\delta^{13}C=-16.0\%$ $\pm~0.4\%$ and F $\sim\!0.0043\,\pm~0.0003$. As noted, this evolved CO_2 component appears to be derived from occluded CO_2 released from the gibbsite sample only during dehydration (i.e., destruction of the gibbsite crystal structure).

4. SUMMARY AND CONCLUSIONS

Incremental vacuum dehydration-decarbonation analyses of a relatively pure gibbsite from an Eocene-age bauxite build on the discovery by Schroeder and Melear (1999) of CO₂ occluded in modern soil-formed gibbsites. The only detectable mineralogical phases present in the Eocene sample are gibbsite with minor amounts of kaolinite and boehmite. There is no evidence

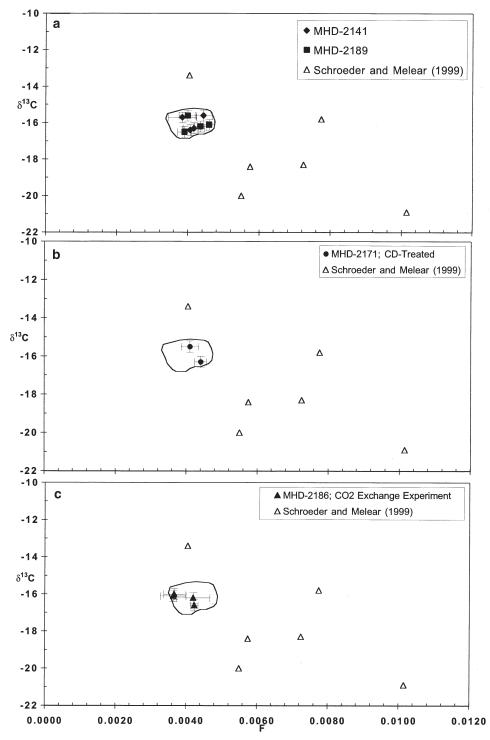


Fig. 5. Plots of δ^{13} C vs. F for incremental dehydration-decarbonation of the Eocene-age gibbsitic bauxite. In plots (a) through (c), F ratios and δ^{13} C values of CO₂ evolved from Holocene-age soil gibbsites reported in Schroeder and Melear (1999) are also shown for comparison (open triangles). Note that Schroeder and Melear (1999) reported C/H ratios for their gibbsite samples as twice the average ratio of moles of CO₂ to moles of H₂O, whereas F values are plotted here as moles of CO₂ to moles of H₂O. The F values for the data of Schroeder and Melear (1999) are one half of the values reported in their paper. (a) Plot of plateau δ^{13} C vs. F values from gibbsite over the "plateau interval" (X_v (H₂) = 0.16–0.67) in experiments MHD-2141 and MHD-2189(0.5N HCl and H₂O₂ treatment only, see text). These data (filled diamonds and squares) define the reference "plateau domain" encompassed by the closed loop. (b) "Plateau interval" δ^{13} C values plotted against F (filled circles) for bauxitic gibbsite that underwent CD treatment (see text) before incremental vacuum dehydration-decarbonation (MHD-2171). The filled circles of MHD-2171 plot within the reference domain (see text). (c) δ^{13} C vs. F values (filled triangles) for increments of CO₂ from the "plateau interval" (X_v (H₂) = 0.16–0.67) for the gibbsitic bauxite (MHD-2186) after the CO₂ exchange experiment. The filled triangles of MHD-2186 plot within the reference plateau domain (see text).

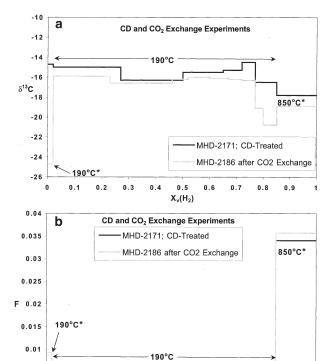


Fig. 6. Incremental dehydration-decarbonation spectra for samples from the CD (MHD-2171) and CO $_2$ exchange (MHD-2186) experiments. For the increments that lie within the "plateau dehydration interval," $X_{\nu}(H_2)=0.16$ to 0.67, for MHD-2171 and MHD-2186, average $\delta^{13}C_{CO_2}$ values are $-16.0\pm0.6\%_0$ and $-16.4\pm0.3\%_0$, respectively, whereas average plateau F values are 0.0043 \pm 0.0002 and 0.0040 \pm 0.0003, respectively.

 $X_v(H_2)$

0.6 0.7

0.8 0.9

0.005

0.1

0.2

for interference from "non-stoichiometric" hydrogen in the 190°C dehydration of the gibbsite in the Eocene bauxite.

 δ^{13} C and F values measured for CO₂ from the 190°C open-system vacuum increments exhibit narrow ranges indicative of their respective "plateaus," which are thought to represent the CO₂ occluded in the gibbsite. The gibbsite plateau δ^{13} C value is $-16.0 \pm 0.4\%$, whereas the plateau F value is 0.0043 ± 0.0003 . A CO₂ exchange experiment at 105°C appears to have had no measurable effect upon these plateau values, indicating that the occluded CO₂ is closed with respect to this process on laboratory time scales. It also appears that CD-treatment has a minimal effect on the δ^{13} C or F values of CO₂ occluded in gibbsite. However, because of the relatively small difference (2.8‰) in δ^{13} C between citrate and CO₂ from gibbsite, we cannot rule out the possibility that citrate sorbed to the gibbsite surface may have affected some of the CO₂ increments evolved during open system dehydration.

The results presented here affirm the hypothesis of Schroeder and Melear (1999) that "plateau" increments of CO_2 evolved during gibbsite breakdown are derived from a non-exchangeable, mineral-bound CO_2 that is only evolved from the mineral phase when the confining gibbsite crystal structure is destroyed. Therefore, CO_2 contained in ancient gibbsites may provide a mineralogical archive of terrestrial carbon budgets and paleo-

 CO_2 concentrations comparable to that found in goethite and calcite

The two parameters of potential paleoenvironmental significance obtained from the gibbsite in this work (F and δ^{13} C) have values of 0.0043 \pm 0.0003 and $-16.0 \pm 0.3\%$. Until the value of the carbon isotope fractionation factor (α) between CO₂ in gibbsite and CO₂ gas, as well as values for a Henry's Law-type distribution coefficient, are known, there are limits to what can be deduced about the carbon system present in the Eocene soil. However, using the tentative estimate of Schroeder and Melear (1999) for α (\sim 1.000), the soil CO₂ present at the time of crystallization of gibbsite seems to have had a δ^{13} C value of about -16.0%. Such a value would indicate a possibly significant contribution of CO₂ from the atmosphere and/or dissolving calcite in a soil containing oxidizing organic matter (e.g., Yapp and Poths, 1991; 1992; Hsieh and Yapp, 1999; Yapp, 2001; Tabor et al., 2004).

The full paleoenvironmental significance of plateau values of $\delta^{13}C$ and F of CO_2 occluded in gibbsite will become more apparent if controlled gibbsite synthesis experiments can provide refined estimates of α and determine the Henry's Law coefficient between ambient CO_2 and CO_2 occluded in gibbsite. Once the values of these two parameters have been determined, the plateau $\delta^{13}C$ and F values of CO_2 occluded in gibbsite may ultimately be used to infer ancient soil carbon budgets, soil productivity, soil and atmospheric Pco_2 concentrations.

Acknowledgments—We thank Tim Lowenstein, Paul Knauth, and two anonymous reviewers for helpful comments. This work was funded by NSF Grant EAR-0106257 to C.J. Yapp.

Associate editor: T. Lowenstein

REFERENCES

Bird M. I., Longstaffe F. J., Fyfe W. S., Tazaki K., and Chivas A. R (1994) Oxygen isotope fractionation in gibbsite; synthesis experiments versus natural samples. *Geochim. Cosmochim. Acta* 58, 5267–5277.

Craig H. (1957) Isotopic standards for carbon and oxygen and correction factors for mass-spectrometric analysis of carbon dioxide. Geochim. Cosmochim. Acta 12, 133–149.

Criado J. M, Ortega A., Real C., and Torres de Torres E. (1984) Re-examination of the kinetics of the thermal dehydroxylation of kaolinite. Clay Min. 19, 653–661.

Girard J. P., Freyssinet P., and Morillon A. C. (2002) Oxygen isotope study of Cayenne duricrust paleosurfaces; implications for past climate and laterization processes over French Guiana. *Chem. Geol.* 191, 329–343.

Gordon M., Tracey J. I. and Ellis M. W.(1958) Geology of the Arkansas bauxite region. U.S.G.S., Prof. Papers 299, 268pp.

Hsieh J. C. C., and Yapp C. J. (1999) Stable carbon isotope budget of CO₂ in a wet, modern soil as inferred from Fe(CO₃)OH in pedogenic goethite: Possible role of calcite dissolution. *Geochim. Cosmochim. Acta* 63, 767–783.

Jackson M. L. (1979) Soil Chemical Analysis-Advanced Course. Published by the Author, Madison, Wisconsin.

Moore D. M., and Reynolds R. C. Jr (1997) X-Ray Diffraction and the Identification and Analysis of Clay Minerals, 2nd ed., Oxford University Press, New York, 378 p.

Paulik F., Paulik J., Naumann, R., Kohnke, K., and Petzold D. (1983) Mechanism and kinetics of the dehydration of hydrargillites. Part 1Thermochim. Acta 64, 1–14.

Rooksby H. P. (1961) Oxides and hydroxides of aluminum and iron. In The X-ray identification and Crystal Structures of Clay Minerals (ed. G. Brown), pp. 354–392. Mineralogical Society, London

- Schroeder P. A., and Melear N. D. (1999) Stable carbon isotope signiatures preserved in authigenic gibbsite from a forested granitic-regolith: Panola Mt., Georgia, USA. Geoderma 91, 261–279.
- Tabor N. J., Yapp C. J., and Montanez I. P. (2004) Goethite, calcite, and organic matter from Permian and Triassic soils: carbon isotopes and CO₂ concentrations. *Geochim. Cosmochim. Acta* 68, 1503–1517.
- Valeton I. (1972) Bauxites. Developments in Soil Science 1, Elsevier, New York, 226 pp.
- Vitali F., Longstaffe F. J., Bird M. I., Gage K. L., Caldwell W. G. E. (2001) Hydrogen isotope fractionation in aluminum hydroxides; synthesis products versus natural samples from bauxites. *Geochim. Cosmochim. Acta* 65, 1391–1398.
- Yapp C. J. (1983) Stable hydrogen isotopes in iron oxides—isotope effects associated with dehydration of natural goethite. *Geochim. Cosmochim Acta* 47, 1277–1287.
- Yapp C. J. (1987) A possible goethite-iron (III) carbonate solid solution and the determination of CO₂ partial pressures in low temperature geologic systems. *Chem. Geol.* **64**, 259–268.
- Yapp C. J. (1996) The abundance of Fe(CO₃)OH in goethite and a possible constraint on minimum atmospheric oxygen partial pressures in the Phanerozoic. *Geochim. Cosmochim Acta* 60, 4397– 4402
- Yapp C. J. (1998) Paleoenvironmental interpretations of oxygen isotope ratios in oolitic ironstones. *Geochim. Cosmochim Acta* 62, 2409–2420.

- Yapp C. J. (2001) Mixing of CO₂ in Surficial Environments as Recorded by the Concentration and δ¹³C Values of the Fe(CO₃)OH Component in Goethite. *Geochim. Cosmochim. Acta* **65**, 4115–4130.
- Yapp C. J., and Pedley M. (1985) Stable hydrogen isotopes in iron oxides—II. D/H variations among natural goethites. *Geochim. Cos*mochim. Acta 49, 487–495.
- Yapp C. J., and Poths H. (1990) Infrared spectral evidence for a minor Fe(III) carbonate-bearing component in natural goethite. *Clays Clay Min.* **38**, 442–444.
- Yapp C. J., and Poths H. (1991) ¹³C/¹²C ratios of the Fe(III) carbonate component in natural goethites. In *Stable isotope geochemistry: A tribute to Samuel Epstein* (ed. H. P. Taylor Jr. et al.); Geochemical Society Special Publication 3,257–270
- Yapp C. J., and Poths H. (1992) Ancient atmospheric CO₂ pressures inferred from natural goethites. *Nature* 355, 342–344.
- Yapp C. J., and Poths H. (1993) The carbon isotope geochemistry of goethite (α-FeOOH) in ironstone of the Upper Ordovician Neda Formation, Wisconsin, USA: Implications for early Paleozoic continental environments. *Geochim. Cosmochim. Acta* 57, 2599–2611.
- Yapp C. J., and Poths H. (1996) Carbon isotopes in continental weathering environments and variations in ancient atmospheric CO₂ pressure. *Earth Planet. Sci. Lett.* 137, 71–82.

APPENDIX 1

Bauxite (MHD-2128) HCL + H ₂ O ₂		CO ₂		Sample mass $^1 = 109.2 \text{ mg}$		
Time (min)	T (°C)	μmoles	$\delta^{13}C$	${ m H_2}~\mu{ m moles}$	$X_v(H_2)$	F
61 + 30	25 + 100	0.1	-9.5	59	N/A	N/A
30	230*	6.4	-15.7	1016	0.55	0.0063
30	230	1.4	-15.7	510	0.83	0.0027
31	230	0.4	-18.7	28	0.84	0.0143
30	230	0.4	-18.7	25	0.86	0.0160
30	230 - 245	0.5	-16.8	37	0.88	0.0135
31	850*	9.7	-17.9	225	1.00	0.0431
Bauxite (MHD-2141) HCl + H ₂ O ₂		CO ₂		Sample $mass^1 = 179.3 \text{ mg}$		
Time (min)	T (°C)	μ moles	$\delta^{13}C$	H_2 μ moles	$X_v(H_2)$	F
26 + 30	23 + 100	0.2	-8.4	77	N/A	N/A
30	190*	0.6	-15.6	70	0.02	0.0086
30	190	1.7	-15.2	419	0.16	0.0041
31	190	1.9	-16.4	467	0.32	0.0041
30	190	1.8	-15.6	405	0.45	0.0044
30	190	1.4	-16.3	336	0.55	0.0042
31	190	1.0	-15.7	260	0.65	0.0038
33	190	0.7	-16.3	203	0.71	0.0034
36	190	0.5	-16.0	142	0.76	0.0035
128	190	0.5	-18.4	187	0.82	0.0027
30	850*	17.3	-18.7	544	1.00	0.0318

Bauxite (MHD-2171) $CD + HCl + H_2O_2$		CO ₂		Sample $mass^1 = 171.7 \text{ mg}$		
Time (min)	T (°C)	μ moles	$\delta^{13}C$	H_2 μ moles	$X_v(H_2)$	F
165 + 57	25 + 100	0.1	-12.8	337	N/A	N/A
30	190*	0.4	-14.7	66	0.02	0.0061
30	190	3.4	-15.0	685	0.27	0.0050
30	190	2.8	-16.3	635	0.50	0.0044
30	190	1.7	-15.5	415	0.65	0.0041
30	190	0.8	-15.3	213	0.72	0.0038
60	190	0.4	-14.5	126	0.77	0.0032

APPENDIX	1	(Continued)

		APPI	ENDIX 1 (Continue	d)			
Bauxite (MHD-2171) CD + HCl + H ₂ O ₂		CO ₂		Sample $mass^1 = 171.7 \text{ mg}$			
Time (min)	T (°C)	μ moles	$\delta^{13}C$	H_2 μ moles	$X_v(H_2)$	F	
1050 30	190 850*	0.7 14	-16.5 -17.8	230 412	0.85 1.00	0.0030 0.0340	
Bauxite (MHD-2186) CO ₂ Exchange HCl + H ₂ O ₂		CO ₂		Sample $mass^1 = 234.0 \text{ mg}$			
Time (min)	T (°C)	μ moles	$\delta^{13}C$	H_2 μ moles	$X_v(H_2)$	F	
60 + 110 3875	22 + 100 100	0.4 863 ²	-9.5 -45.8	110 0	Tank	Before CO ₂ Exchange Tank CO ₂	
40 . 20	After CO ₂	exchange, sample was	removed and treate	ed with 0.5N HCl, 30% H	1 ₂ O ₂	27/1	
48 + 30	22 + 100	0.1	-26.5	113	N/A	N/A	
36	190*	0.9	-24.7	98	0.02	0.0092	
30	190	3.9	-15.9	832	0.23	0.0047	
30	190	3.9	-16.6	922	0.46	0.0042	
31	190	0.9	-16.2	214	0.52	0.0042	
30	190	1.2	-16.0	327	0.60	0.0037	
30	190	1.0	-16.1	275	0.67	0.0036	
30	190	0.5	-16.2	197	0.72	0.0025	
45	190	0.4	-16.3	183	0.77	0.0022	
77	190	0.2	-19.1	147	0.80	0.0014	
885	190	1.0	-20.8	164	0.85	0.0060	
30	850*	21.9	-18.9	614	1.00	0.0357	
Bauxite (M			_	~			
$\underline{\hspace{1cm}} HCl + H_2O_2$		$\underline{\hspace{1cm}}^{\hspace{1cm}} \operatorname{CO}_2$		Sample mass $^1 = 254.9 \text{ mg}$			
Time (min)	T (°C)	μmoles	δ^{13} C	H_2 μ moles	$X_v(H_2)$	F	
43 + 35	22 + 100	0.3	-8.2	97	N/A	N/A	
30	190*	0.8	-16.0	103	0.02	0.0078	
30	190	2.8	-15.4	591	0.16	0.0047	
30	190	3.1	-16.1	675	0.31	0.0046	
30	190	2.7	-16.2	621	0.45	0.0043	
30	190	2.0	-16.5	512	0.57	0.0039	
30	190	1.6	-15.6	400	0.66	0.0040	
30	190	0.8	-16.0	273	0.72	0.0029	
30	190	0.3	-16.7	189	0.77	0.0016	
33	190	0.2	-16.8	113	0.79	0.0018	
38	190	0.1	-18.2	74	0.81	0.0014	
30	850*	24.5	-19.2	835	1.00	0.0293	

^{*} Closed system in O_2 .

¹ Sample masses are after 100°C outgassing.

² After 100°C outgassing of MHD2186, sample was left in closed system with 0.10atm CO_2 . This fraction is the CO_2 present in the 105°C atmosphere after 3875 minutes. See text for further discussion.